Available online at www.sciencedirect.com

ScienceDirect

Procedia Engineering 157 (2016) 325 – 332

Procedia Engineering

www.elsevier.com/locate/procedia

IX International Conference on Computational Heat and Mass Transfer, ICCHMT2016

Characterization of Defects in Curved Composite Structures Using Active Infrared Thermography

Przemysław Daniel Pastuszak*

Institute of Machine Design, Faculty of Mechanical Engineering, Cracow University of Technology, al. Jana Pawła II 37, 31-864 Cracow, Poland

Abstract

The paper presents thermographic studies of curved composite panels (GFRP) with subsurface defects. Two types of defects are analysed: 1) artificial, created by inserting Teflon stripe between individual layers of a laminate during manufacturing stage and 2) real, caused by static loading tests.

The phenomena observed during the experiments can be successfully simulated by means of the FEM which considerably expands capabilities of standard AIRT. ANSYS package was used to simulate transient heat transfer in 3D model with embedded various defects. Results confirmed the validity of the FE model in comparison to conducted experiments.

Analysis of temperature distribution on investigated surfaces provides the opportunity to determine the geometry of subsurface defects.

Peer-review under responsibility of the organizing committee of ICCHMT2016

Keywords: Active Infrared Thermography; Curved Composite Structures; Defects.

1. Introduction

The exponential development of science and technology determines changes in the way of the design of engineering structures. Rising of already strict strength criteria simultaneously with constant lowering the weight and the volume of constructions involve a need for optimal usage of existing materials, but above all the creation of new and hitherto unique compositions. Alternative to traditional isotropic materials are multilayered composites which thermo-mechanical properties can be tailored directionally according to the arrangement of layers. Unfortunately,

* Corresponding author. Tel.: +48 12 628 33 05; fax: +48 012 374 33 60.
E-mail address: ppastuszak@pk.edu.pl

Peer-review under responsibility of the organizing committee of ICCHMT2016
doi:10.1016/j.proeng.2016.08.373

despite a number of significant advantages of composite materials, they are prone to various modes of failures, such as fiber breakage, fiber debonding, matrix cracking and the delamination. These failure mechanisms can interact each other and develop, significantly lowering properties of the structural components. Presence of defects in elements made of the composite materials increase their manufacturing costs and/or elongate the out of service time. Additionally, there is high probability, that in many cases internal flaws remain undetected, which can result in the risk of the human health or life. Therefore, there is demand for development of the cost-effective Non-Destructive Testing methods (NDT) for the detection and evaluation of the subsurface defects in multilayered composite structures in the manufacturing stage or subsequent maintenance.

Infrared Thermography has several advantages in comparison with other of NDT methods such as ultrasonic testing [1]. It is fast, noncontact, has wide range of applications, can be single-sided and offers large area coverage. Furthermore, this non-invasive method creates opportunities to apply it practically in any process where the temperature is indicator of the abnormal operation of the object. It should be also noted that fibrous composites are considered as the very successful targets for the application of Active Infrared Thermography (AIRT) due to their thermal and emissive properties.

Generally, active IR thermography (AIRT) uses a thermal excitation source (eg. heating by halogen lamp or high-power flashlight) to heat the surface of the investigated component, then, a highly sensitive infrared camera records series of thermograms at regular intervals of time. Contrary to FT mode where heating or cooling time equals few milliseconds (e.g. about 40 ms for 2 mm thick aluminium specimen) and the temperature decay is in the center of interest, during application of LPT procedure, the surface is observed both during heating and cooling stages for few seconds to minutes (depending on material's thermophysical properties). It should also be noted, that the pulse duration must be chosen carefully to prevent failure of investigated materials (eg. danger of investigated object over-heating). The sub-surface flaws affect the way in which heat is conducted into the material, resulting in time-dependent temperature variations on the surface. Results are visualized through the creation of thermal images (thermograms) which map the temperature distribution on the surface of the examined objects [2-4].

Numerous examples has been presented in the literature on the use of thermography to investigate, e.g., hidden corrosion in metallic plates [5], cracks in ceramics [6] or disbonds in reinforced concrete [7]. Interesting field of Infrared Thermography use concerns defect detection and its quantification in high-performance application like aircrafts [8,9]. However, majority of studies are concentrated only on evaluation of defects in composite plates [10-15]. Whereas, composite materials are mostly used in complex components, e.g., pipes, corners and stiffeners [16]. Local decrease of mechanical properties in these regions can have decisive influence on strength of the entire structure. Application of active procedures of thermography to defect detection and evaluation in this type of elements seems to be more appropriate than other NDT techniques. Nevertheless, there are various uncertainties connected with correct interpretation of acquired data.

This work is focused on thermographic studies of curved composite panels (GFRP) with subsurface defects. Two types of defects are analysed: 1) artificial, created by inserting Teflon stripe between individual layers of a laminate during manufacturing stage and 2) real, caused by static loading tests. The analysis is conducted by the comparison of the finite element results with experimental ones. The ANSYS package was used to simulate transient heat transfer in 3D model with embedded various defects.

2. Numerical (Finite Element) modelling

Finite Element Method (FEM) offers capabilities to better understanding of thermal processes, which are the basis of thermographic analysis. The numerical investigation can be conducted in order to simulate the heat flow through the material as well as the stress and strain distributions during loading conditions including both mechanical and thermal loads.

In the present work, transient heat transfer analysis is performed for 3D model with embedded various defect sizes. Examined specimens were analyzed using ANSYS package version 12.1.

Fig. 1 shows boundary conditions and finite element mesh used in this analysis. It was assumed that the investigated specimen was in equilibrium with the environment, therefore measured ambient temperature in the laboratory was used in the numerical model both as a boundary and as initial conditions. Convective coefficient corresponds to value recommended in literature for natural convection in still air environment (h=10). The density

of the heat flux was identified with the use of experimental results. Entire analysis, similarly like in experiment, was 60 seconds (10 seconds heating and 50 second cooling by ambient air).

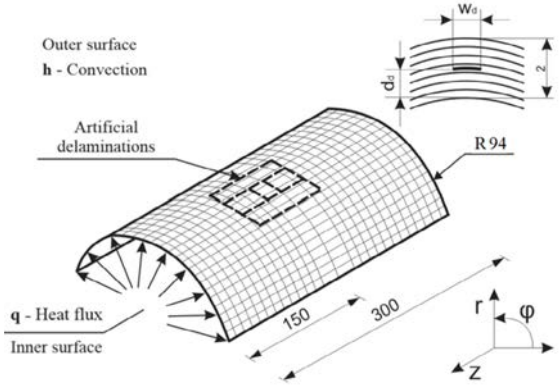

Fig. 1. Geometry and boundary conditions of the 3D numerical model.

SOLID90 3-D high order thermal solid element was used in current investigation. This element has 20 nodes, each of them has one degree of freedom: temperature. It has compatible temperature shapes and is well suited to model curved boundaries [17].

Thermophysical properties of materials used during modelling, were either taken from literature or values specified by producer of investigated material [18-20].

Table 1. Thermophysical properties of used materials during modelling [18-20].

Material	Thermal conductivity λ (W/mK)	Density ρ (kg/m3)	Heat capacity Cp (J/kgK)
GFRP (⊥ fibre)	0.3	2221.6	747.77
GFRP (∥ fibre)	0.38		
Teflon	0.1	2150	1043

3. Experimental work

The specimens were manufactured from 8 plies of Hexcel TVR 380 M12/R-glass unidirectional prepreg layers. The geometry of specimens was cylindrical with a nominal thickness equal 2 mm, the length 300 mm and the inner radius 92 mm (Fig. 2a). The laminate had a nominal fibre volume of 60% and the ply thickness equals to 0,25mm.

a) b)

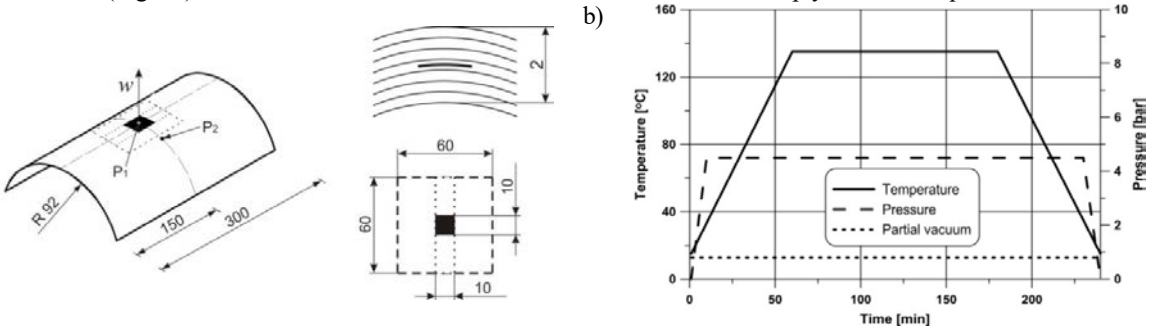

Fig. 2. (a) investigated composite shell with various delaminations; (b) diagram of the manufacturing process of the examined specimens.

To provide compromise between realistic representation and ease of preparation the delamination, Teflon film in the form of a single square was introduced in the manufacturing stage in the middle of the laminate specimens between 4^{th} and 5^{th} layer. Position of these inserts in relation to specimens is shown in Fig. 2a. Additionally, to minimize the end effect and to prevent crushing, both ends of investigated specimens were encased in steel matrices and the epoxy resin.

It was proved in [21], that manufacturing process has great influence on strength properties and load carrying capacity of the thin-walled composite structures. Therefore, in order to ensure high quality of the specimens and repeatability of the manufacturing process, all laminates were cured in the autoclave at optimal conditions: 135 °C for 120 min at 4,5 bar of the pressure and 0,8 bar of the partial vacuum. Additionally, to minimize the residual stresses generated during the production and arising from the anisotropy of the thermal expansion of the composite materials, heating and cooling stages were done at 2 °C per minute. This process is schematically illustrated in Fig. 3b.

All investigated specimens had three types of the stacking sequence denoted as A, B, C or D configurations with different sizes and thicknesses of the delaminations. Details are described in

Table 2. Configurations of the examined specimens.

Denotation	Stacking sequence	Geometry of a delamination [mm]	Thickness of a delamination [μm]
A	$[0/90/0/90]_s$	Square 60x60	50
B	$[0/90/0/90]_s$	Rectangular 10x60	50
C	$[90]_8$	Square 10x10	400
D	$[0]_8$	Square 10x10	400

The system used in this study consists of Flir A325 camera with a frame rate of 60 Hz and a focal plane array pixel format of 320x240, the halogen lamp, the computer and the trigger box. The entire process is controlled by using IR-NDT software. The same program is used to the processing of the acquired data. Fig. 3a shows the complete experimental setup used in the current investigation. To monitor possible delamination growth increment, specimens can be subjected to the thermographic analysis during each step of loading. Furthermore, tests were monitored using a standard camera.

a) b)

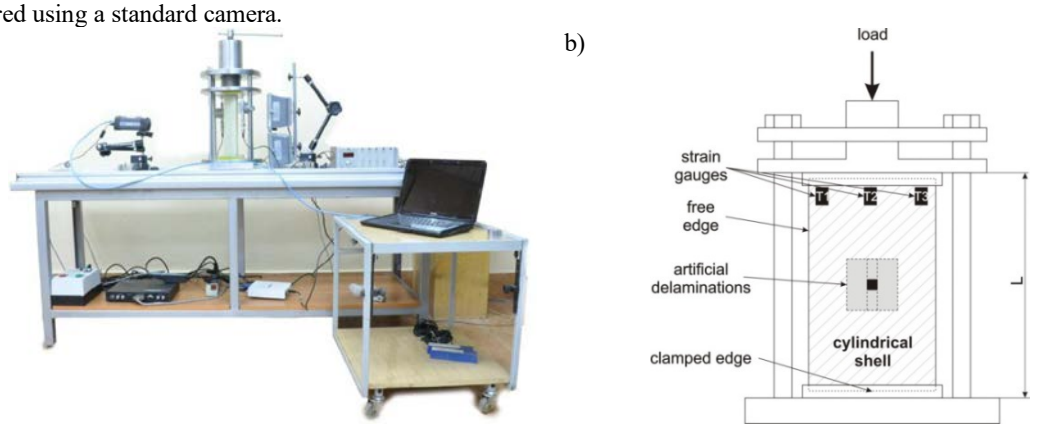

Fig. 3. (a) experimental setup; (b) the loading test apparatus for the two-edge clamped boundary condition.

The cylindrical panels were also tested in an loading machine with manual displacement control. In all tests, the load was applied in the axial direction at ambient conditions. Each examined specimen was instrumented with three strain gauges in order to evaluate uniformity of load. The data was acquired and processed throughout the tests by measuring amplifier HBM MGCplus and personal computer with the dedicated software CATMAN. Configuration of the loading test apparatus is presented in Fig. 3b.

4. Results and discussion

4.1. Effects of the artificial delamination

First part of this work was devoted to the detection and location of the artificial damage for the unloaded structure. For this purpose a Pulsed Infrared Thermography method was used. Additionally, based on the distribution of temperatures in selected areas, thickness and sizes of the embedded defects was evaluated. Due to great amount of acquired data, only selected results are presented here. Fig. 4 shows the representative thermograms obtained during the heating of the unloaded specimens with the inserted defects for A&C investigated configurations. In the thermal image of the A configuration, shape of the artificial delamination is barely visible unlike to the C configurations where rectangular shape of artificial defect can be easily detect.

The detection of the temperature variations was observed at two chosen areas: defective and non-defective. The correlation between the changes of the temperature of the specimen and the thicknesses of Teflon inserts can be observed. Fig. 6 demonstrates the temperature evolutions with time at these two areas for A&C configurations of investigated specimens. Obtained temperature contrasts, maximal and minimal temperatures throughout the thermographic analysis of the each run for investigated areas are given in Table 3.

Table 3. Maximal Absolute Thermal Contrast (ATC), initial and maximal temperature for defective and non-defective areas.

Configuration	Initial temperature [°C]	Maximal temperature [°C]	Max ATC [°C]
	Experiment		
A	24,56	48,01	0,60
B	24,85	48,05	0,57
C	24,24	48,13	3,17
D	24,28	48,08	3,01
	FEM		
A&B	24,50	47,57	0,73
C&D	24,50	47,57	3,15

The phenomena observed during the experiments can be successfully simulated by means of the FEM as it may be observed in Fig. 6. Abnormal distribution of the temperature on the investigated outer surface of the 3D numerical model of the cylindrical panel is caused by presence of the artificial delamination in the structure. The temperature contrast are induced by the different thermal properties of the composite material and the inserted artificial delamination. In essence, owing to these differences, it is possible to reveal subsurface discontinuities. It can be seen that numerical results show good correlation with experimental ones – Table 3.

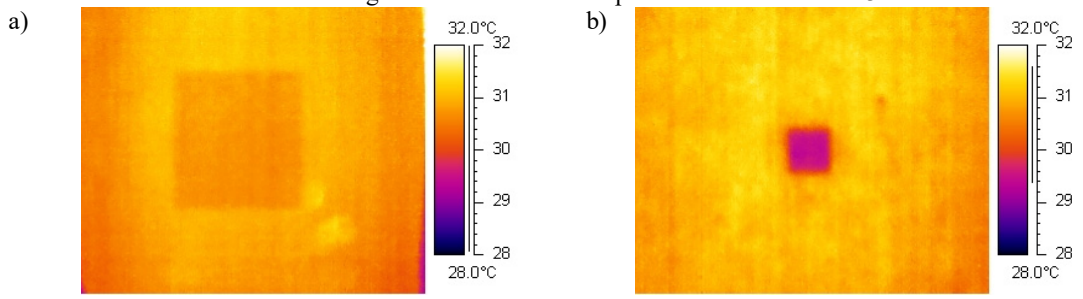

Fig. 4. Thermograms of the unloaded specimens with the embedded defects for (a) A configuration and (b) C configuration.

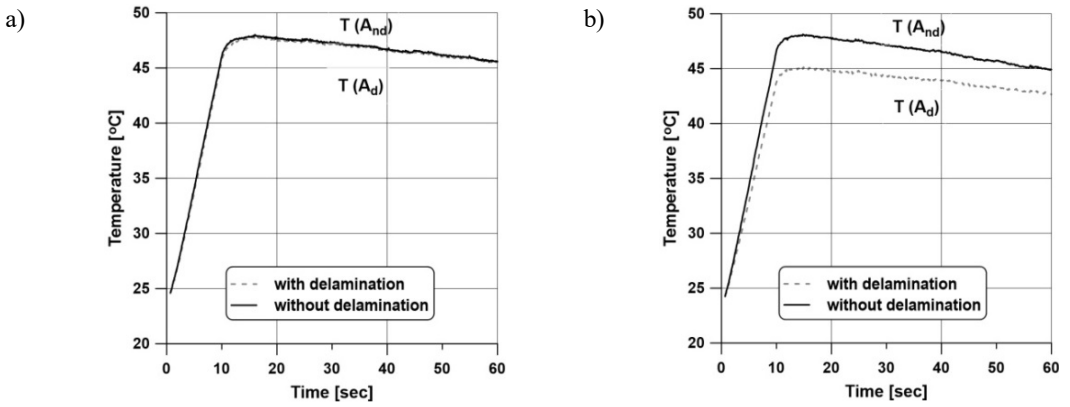

Fig. 5. Temperature variations versus time for (a) A configuration and (b) C configuration.

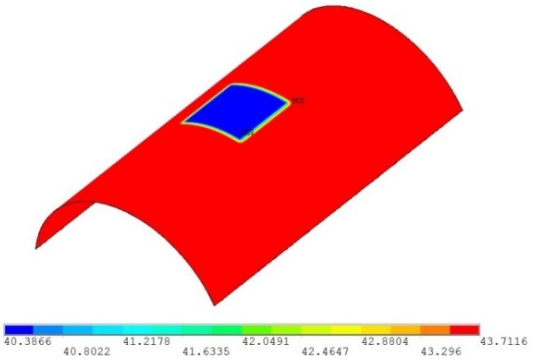

Fig. 6. Temperature distribution on the outer surface of investigated 3D numerical model of the cylindrical panel with delamination for A configuration.

4.2. Effects of the delamination growth

Further analysis was carried out under various loading condition represented by the values of the displacements of the boundary plates measured in mm, since the cylindrical panel was compressed in order to investigate the opening of the artificially delaminated area. Values respectively for examined configurations giving in Table 4 describes the critical end-shortening of the sample when it does not carry the load any more.

Table 4. Values of the Critical end-shortening of the investigated specimens.

Denotation	Stacking sequence	Critical end-shortening value [mm]
A	$[0/90/0/90]_s$	2,39
B	$[0/90/0/90]_s$	3,05
C	$[90]_8$	1,43
D	$[0]_8$	1,50

For B, C and D configurations, artificially introduced delamination was not expands during compressive mechanical loading till the final failure, therefore to the further considerations, the most interesting example in the form of A Configuration will be presented.

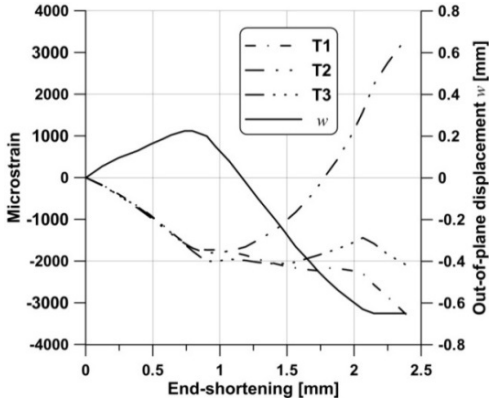

Fig. 7. Variations of the strains and the out of plane displacement as a function of the end-shortening for A configuration.

Next step of the investigation concerned analysis of the strains variation and the out of plane displacement w in the center of the artificial delamination – Fig. 2a. Arrangement of the strain gauges: T1, T2 and T3, is presented in Fig. 3b. Comparison between the measured microstrains and the out of plane displacements as a function of the end-shortening is given in Fig. 7. One can observe that uniform distribution of load is provided up to 1mm.

Fig. 8a provides thermal image of the final failure form of the A configuration specimen. It is clearly seen that propagation of the artificial delamination within the specimen is not uniform, therefore, thermogram have been divided into three areas denoted as A1, A2 and A3 with different level of the defected region.

The correlation between the temperature variations of the selected areas and the level of the damage can be observed – see Fig. 8b. The most delaminated region has the lowest temperature distribution (A3) in contrast to the less damaged (A1). According to the prior consideration it is caused by different thermal properties of composite materials, Teflon insert, voids of air (real delamination) and the interactions of the various failure mechanisms occurring in fibrous composite materials.

a) b)

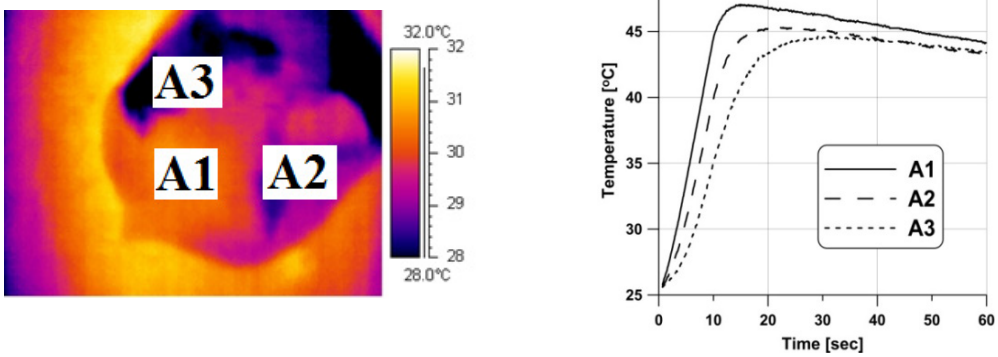

Fig. 8. (a) thermogram of the loaded specimen with the defects for A configuration; (b) temperature variation versus time for three selected areas of A configuration for end-shortening equals 2,39 mm.

5. Conclusions

The present study emphasized the ability of the Pulsed Thermography to detect, locate and evaluate of the delamination (artificial and developed during the static tests) within GFRP cylindrical panels with different stacking sequences and subjected to an axial compression.

The obtained results proved the effectiveness of used technique and provide further information for active infrared thermography as a viable nondestructive evaluation tool for testing of curved composite structures. The phenomena observed during the experiment can be successfully simulated by means of the FEM. More extensive numerical results will be presented in the further work.

In addition, it was noted that despite of anisotropic nature of investigated specimens, influence of the stacking sequence to detection of the delamination is negligible for present PT method.

Acknowledgements

The research project DEC-2013/09/N/ST8/04360 was funded by the National Science Centre in Poland.

References

[1] J. Bieniaś, P. Jakubczak, K. Majerski, M. Ostapiuk, B. Surowska, Methods of ultrasonic testing, as an effective way of estimating durability and diagnosing operational capability of composite laminates used in aerospace industry, Eksploatacja i Niezawodność – Maintenance and Reliability, 15 (3) (2013) 284–289.

[2] X.P.V. Maldaque, Theory and practice of infrared technology for nondestructive testing, John Wiley & Sons, Inc., New York – Toronto, 2001.

[3] P.D. Pastuszak, A. Muc, M. Barski, Methods of infrared non-destructive techniques: review and experimental studies, Key Engineering Materials 542 (2013) 131-141.

[4] A. Muc, P.D. Pastuszak, Evaluation of subsurface defects in cylindrical composite structures using active thermography, Proceedings of the 16th European Conference on Composite Materials, Sewilla, Spain, 2014.

[5] D. Wu, G. Busse, Lock-in thermography for nondestructive evaluation of materials, Revue Generale de Thermique, 37 (8) (1996) 693–703.

[6] D. Wu, et al., Nondestructive inspection of turbine blades with lock-in Thermography, Materials Science Forum 210–213 (1996) 289–294.

[7] M.R. Valluzzi, E. Grinzato, C. Pellegrino, C. Modena, IR thermography for interface analysis of FRP laminates externally bonded to RC beams, Materials and Structures, 42 (2009) 25–34.

[8] T.D. Orazio, C. Guaragnella, M. Leoa, P. Spagnolo, Defect detection in aircraft composites by using a neural approach in the analysis of thermographic images, NDT&E International, 38 (2005) 665–673.

[9] N.P. Avdelidisa, D.P. Almond, A. Dobbinson, B.C. Hawtinb, C. Ibarra-Castanedo, X. Maldague, Aircraft composites assessment by means of transient thermal NDT, Progress in Aerospace Sciences 40 (2004) 143–162.

[10] K. Ghadermazi, M.A. Khozeimeh, F. Taheri-Behrooz, M.S. Safizadeh, Delamination detection in glass–epoxy composites using step-phase thermography (SPT), Infrared Physics & Technology 72 (2015) 204–209.

[11] V. Feuillet, L. Ibos, M. Fois, J. Dumoulin, Y. Candau, Defect detection and characterization in composite materials using square pulse thermography coupled with singular value decomposition and analysis and thermal quadrupole modeling, NDT&E International 51 (2012) 58–67.

[12] N.P. Avdelidis, D.P. Almond, Z.P. Marioli-Riga, A. Dobbinson, B.C. Hawtin, Pulsed thermography: philosophy, qualitative & quantitative analysis on aircraft materials & applications, Proc. Vth International Workshop, Advances in Signal Processing for Non Destructive Evaluation of Materials Québec City (Canada), 2005.

[13] X. Maldague, A. Ziadi, M. Klein, Double pulse infrared thermography, NDT&E International 37 (2004) 559–564.

[14] L.D. Tomić, J.M. Elazar, Pulse thermography experimental data processing by numerically simulating thermal processes in a sample with periodical structure of defects, NDT&E International 60 (2013) 132–135.

[15] S. Vallerand, X. Maldague, Defect characterization in pulsed thermography: a statistical method compared with Kohonen and Perceptron neural networks, NDT&E International 33 (2000) 307-315.

[16] P.D. Pastuszak, A. Muc, Application of Composite Materials in Modern Constructions, Key Engineering Materials 542 (2013) 119-129.

[17] Ansys, Inc., Element Reference, Release 12.1, November 2009.

[18] G.K. Vijayaraghavan, S. Sundaravalli, Analysis of delaminations in GRP pipes using infrared thermography, LAP LAMBERT Academic Publishing, Germany, 2010.

[19] Ibarra-Castanedo, C., 2005, Quantitative subsurface defect evaluation by pulsed phase thermography: depth retrieval with the phase, PhD dissertation, Laval University, Quebec City, Canada.

[20] A. Muc, P.D. Pastuszak, Prediction of subsurface defects through a pulse thermography, Proceedings of the 15th European Conference on Composite Materials, Venice, Italy, 2012.

[21] J. Bieniaś, A. Gliszczyński, P. Jakubczak, T. Kubiak, K. Majerski, Influence of autoclaving process parameters on the buckling and postbuckling behaviour of thin-walled channel section beams, Thin-Walled Structures 85 (2014) 262–270.